Crystal Structure and Magnetic Properties of Nanosized $Y_3Fe_5O_{12}$ Epitaxial Layers for Microwave Applications

By using laser molecular beam epitaxy, nanometer size yttrium iron garnet ($Y_3Fe_5O_{12}$, YIG) layers have been grown on gadolinium gallium garnet ($Gd_3Ga_5O_{12}$, GGG) [1 1 1]-oriented substrates. Atomic force microscopy revealed remarkably flat step-and-terrace surface morphology with step height of 1.8 Å characteristic of YIG(1 1 1) surface. Structural studies by electron and X-ray diffraction showed that YIG layer is epitaxial and pseudomorphic to the substrate. Analysis of spatial distribution of X-ray diffraction intensity, which was measured at BL-3A provided useful information for understanding important specific features of epitaxial growth of YIG nanosized films. X-ray magnetic circular dichroism (XMCD) measurements at BL-16A enabled site-selective magnetometry.

Yttrium iron garnet (YIG, $Y_3Fe_5O_{12}$) films are used in microwave devices for many years. Recently it has been shown [1] that in thin (<100 nm) films a substantial reduction of spin wave damping constant can be expected, that is of considerable interest for modern microwave devices. In present work, YIG layers on (1 1 1) gadolinium gallium garnet ($Gd_3Ga_5O_{12}$, GGG) substrate were grown by Laser-Molecular Beam Epitaxy. Various growth parameters were used (substrate temperature, oxygen pressure, film thickness). To minimize spin wave relaxation, YIG films with ultra flat interfaces, controlled stress and stoichiometry have been grown. **Fig. 1a** shows surface morphology of typical ultra flat YIG film with well-pronounced atomic steps on the surface.

To study crystal structure, growth induced film stress and interface layer X-Ray diffraction patterns were measured at BL-3A, **Fig. 1b**. The diffraction pattern from the YIG/GGG(1 1 1) heterostructure is a set of round shape substrate reflections and streaks from YIG film. Diffraction intensity along the streaks is modulated by Laue oscillations. Measurements of both specular and non-specular reflections as well as streaks were performed using point Silicon Drift Detector (SDD) and 2D PILATUS 100K detector. After taking series of 2D images, the 3D intensity distribution in the reciprocal space was obtained and analyzed using dedicated software [2]. It was found that in the (1 1 1) plane lattice constant of the substrate and the film coincide, and along the normal ([1 1 1] direction) the YIG film is stretched out. The value of this deformation depends on the growth temperature and the thickness of YIG layer.

Kinematic approximation was used for modeling diffraction intensity distribution along the streaks. This enabled obtaining additional information on the layer structure, more accurate lattice constant values, the gradient of the lattice constants along the substrate normal, the distance between last plane of the substrate and first plane of the layer, as well as the interface roughness. It was found that in YIG layers with the thickness greater than 6 nm, there is a gradient of lattice parameter in direction of the surface normal; the bottom part of the film is less deformed than the top one. It was also found that YIG layers grown at a high temperature are less strained than the layers grown at a lower temperature.

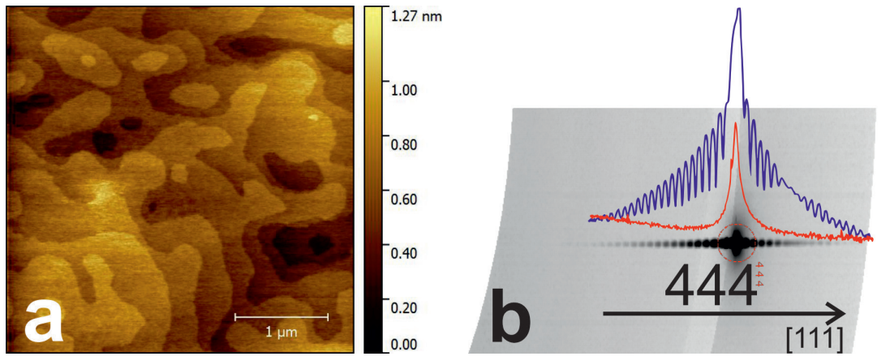

Figure 1: YIG film grown at 1000°C: **(a)** measured by atomic-force-microscopy surface morphology with atomic steps of 1.8 Å; **(b)** X-ray diffraction pattern near YIG and GGG (4 4 4) reflections and intensity distribution along the streak (blue curve) and nearby background (red curve).

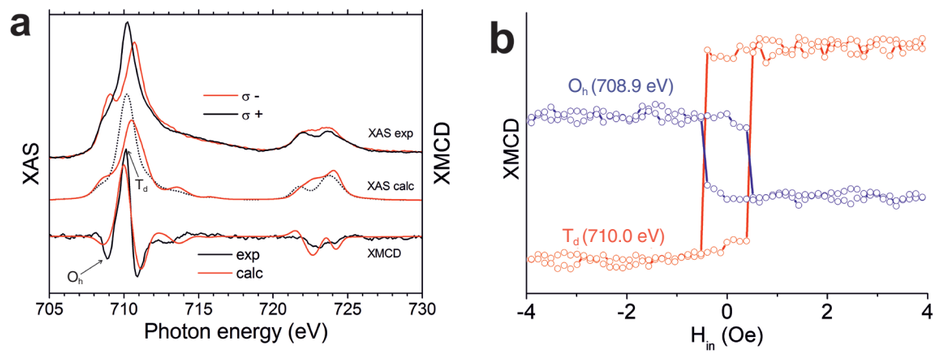

Figure 2: Calculated and experimental XAS and XMCD spectra of YIG film **(a)** and measured by XMCD hysteresis loops for two sublattices formed by iron ions in T_d and O_h sites **(b)**.

In YIG lattice, Fe^{3+} ions are known to occupy tetrahedral (24d) and octahedral (16a) positions forming two anti-parallel magnetic sublattices. Magnetic properties of the films were studied by magneto-optic Kerr effect (MOKE), vibrating sample magnetometer (VSM), ferromagnetic resonance, and XMCD techniques [3-5]. While MOKE and VSM provide information about the total magnetization, XMCD makes it possible to study magnetization of the individual magnetic sublattices.

Figure 2a shows typical XAS and XMCD spectra of YIG film. To analyze contributions of T_d and O_h magnetic sublattices, numerical simulations have been carried out with the use of CTM4XAS software [6]. One can see calculated and experimental curves have very similar characteristic features. Slight difference may be attributed to the charge transfer effects as well as to non-linearity of the measured total-electron-yield signal due to sample charging and saturation effects occurring at high X-ray intensity. It can be also seen from the modeled spectra that by choosing the appropriate photon energy it is possible to make the XMCD measurements to be more sensitive to the magnetization of O_h or T_d sublattice.

At E = 708.9 eV (O_h) XMCD signal is mostly proportional to the octahedral sublattice magnetization while at E = 710 eV (T_d) XMCD probes the sum of octahedral and tetrahedral sublattice magnetizations with main contribution of the tetrahedral one. Magnetization curves measured at these two energies for magnetic field oriented 60° off-the normal are shown in **Fig. 2b**. As expected, the magnetization loops at 708.9 eV and 710 eV are of the opposite sign. The in-plane magnetization curves show very narrow hysteresis loop in agreement with the results of MOKE vector magnetometry [5].

Using data on the crystal quality and growth induced strain of YIG films, as well as their magnetic properties it was possible to optimize the growth conditions of the films for obtaining a record low damping of spin waves [4].

REFERENCES

[1] L. V. Lutsev, *Phys. Rev. B* **85**, 214413 (2012).
[2] S. M. Suturin, A. M. Korovin, V. V. Fedorov, G. A. Valkovsky, M. Tabuchi and N. S. Sokolov, *J. Appl. Cryst.* **49**, 1532 (2016).
[3] N. S. Sokolov, N. S. Sokolov, V. V. Fedorov, A. M. Korovin, S. M. Suturin, D. A. Baranov, S. V. Gastev, B. B. Krichevtsov, K. Yu. Maksimova, A. I. Grunin, V. E. Bursian, L. V. Lutsev, and M. Tabuchi, *J. Appl. Phys.* **119**, 023903 (2016).
[4] L. V. Lutsev, A. M. Korovin, V. E. Bursian, S. V. Gastev, V. V. Fedorov, S. M. Suturin and N. S. Sokolov, *Appl. Phys. Lett.* **108**, 182402 (2016).
[5] B. B. Krichevtsov, S. V. Gastev, S. M. Suturin, V. V. Fedorov, A. M. Korovin, V. E. Bursian, A. G. Banshchikov, M. P. Volkov, M. Tabuchi and N. S. Sokolov, *Sci. Technol. Adv. Mater.* **18**, 352 (2017).
[6] F. M. F. De Groot, J. C. Fuggle, B. T. Thole and G. A. Sawatzky, *Phys. Rev. B* **42**, 5459 (1990).

BEAMLINES

BL-3A and BL-16A

N. S. Sokolov[1], V. V. Fedorov[1], A. M. Korovin[1], L. V. Lutsev[1], S. M. Suturin[1] and M. Tabuchi[2] ([1]Ioffe Institute, [2]SRRC, Nagoya Univ.)